Next Generation Fast Shutter System for LIGO

Thesis by

Kavya Sreedhar

In Partial Fulfillment of the Requirements for the
Degree of
Bachelor of Science in Electrical Engineering

CALIFORNIA INSTITUTE OF TECHNOLOGY
Pasadena, California

2019
Defended June 14, 2019

Kavya Sreedhar
ORCID: 0000-0002-8456-6313

ACKNOWLEDGEMENTS

I would like to thank Richard Abbott for the opportunity to work on an exciting open-ended project. His constant encouragement and advice really made me enjoy research and I found the physics of the problem interesting to understand and fun to play around with. When looking for a research project, I wanted to work on something that took me back to fundamental electricity and magnetism physics that had piqued my interest in electrical engineering in the first place and this project was an ideal fit. Rich's optimism and diligence when solving problems has been inspiring and I hope to approach challenges in the future with the same attitude. This experience was a major factor in my decision to go to graduate school and I am looking forward to it!

I would also like to thank Alan Weinstein in particular for connecting me to Rich. Special thanks to Peter Fritschel, Calum Torrie, Stephen Appert, Dennis Coyne, Charles Osthelder, Eddie Sanchez, Michael Pedraza, Michael Zucker, Julie Hiroto, Alvaro-Miguel Fernandez Galiana, and Nergis Mavalvala for taking the time to think about the Fast Shutter with Rich and me, meeting up for a fun interesting conversations, and welcoming me into the LIGO community.

I also would like acknowledge the National Science Foundation for the grant that funded this project through Award PHY1764464.

ABSTRACT

The proposal for the next generation Fast Shutter system intended to replace the current electromagnetic system used to block an optical pulse that is part of the LIGO observational setup is presented and discussed. The current system setup, problems solved with the new setup, and experiments guiding the new proposal design are detailed along with future work remaining to verify the operation of the next generation Fast Shutter system before it is used in LIGO's observatories.

This system is an electro-mechanical device consisting of two coils of electrically conducting wires and a payload made up of two magnets of opposite polarity configured to move between the upper and lower parts of the device. The mirror is attached to the magnet payload and is used to reflect optical pulses. When a current is applied to the coils, the magnets and attached mirror can move vertically relative to the coils due to the Lorentz force from the current in the coils acting on the magnets. The system can be operated in air or in a vacuum environment over a wide range of temperature and cleanliness requirements.

This system offers a novel and robust solution compared to LIGO's previously patented electro-magnetic ultra-fast shutter due to the design of a moving payload consisting of magnets and a mirror with no wires attached, compared to the prior design consisting of a moving coil requiring electrical attachment. As a result, this system avoids the failure mode associated with wire fatigue caused by repeated flexure of the coil attachment wires. With stationary coils, this system uses permanent magnets for the upward propulsion of the payload. Eddy current damping provided by copper interacting with the payload magnets is included to damp the oscillatory transient response of the payload. This newly designed system achieves the same critical performance specifications as the previously patented ultra-fast mechanical shutter, while being physically smaller, cheaper to build, and vastly more reliable.

TABLE OF CONTENTS

LIST OF ILLUSTRATIONS

LIST OF TABLES

Chapter 1

INTRODUCTION

1.1 Background

The Laser Interferometer Gravitational-Wave Observatory (LIGO) is funded by the National Science Foundation (NSF) and is operated by Caltech and MIT to detect gravitational waves by building robust experiments using laser interferometry. One critical part of the experimental setup is the Fast Shutter aka TOASTR (Turbo Optical Anti-Symmetric Transient Rejector). The Fast Shutter is an electromagnetic system with a reflector payload to block an optical pulse (of up to 45 Joules with a 5 millisecond pulse width) that would damage photodiodes at the anti-symmetric port of the LIGO interferometer with prolonged exposure (Fritschel and Abbott, 2014).

The motivation behind this thesis was to start work on developing the next generation Fast Shutter to replace the current version used in LIGO observatories and more generally, design a high-speed electromagnetic blocking and reflecting mechanism. The below sections will introduce the current system setup to be replaced by the senior thesis work resulting in the development of the more robust next generation Fast Shutter system.

Such a fast electromagnetic blocking mechanism is widely applicable and in high demand. The novelty of this system, especially in comparison to LIGO's previously patented system, is due to the

- design of a moving payload as opposed to moving coil to avoid moving wires that could break when accelerated very quickly
- the optimal allocation of mass between magnet(s) and the mirror for the payload
- use of eddy current damping with copper along with oppositely polarized magnets to bring the payload down to a predetermined vertical blocking position

1.2 First Production Implementation of the Fast Shutter System

The existing Fast Shutter consists of a movable coil with a mirror payload that jumps upward to block the optical pulse when a current pulse is applied to the coil.

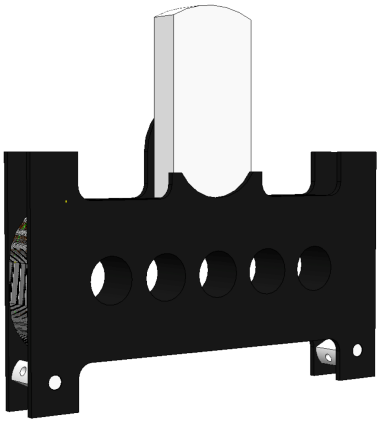

Figure 1.1: Fast Shutter Coil Assembly consisting of PEEK body encasing approximately 300 turns of 32 AWG polyimide-insulated copper wire and a mirror to block the optical pulse from hitting the photodiodes. Figure originally included in (Fritschel and Abbott, 2014).

When the shutter is idle (before the current pulse is applied), the coil is between two pairs of magnets, one pair at the top and one pair at the bottom. When the current pulse is applied, the magnets exert a magnetic force on both the top and bottom of the coil in the same direction, resulting in a net force in the upward direction.

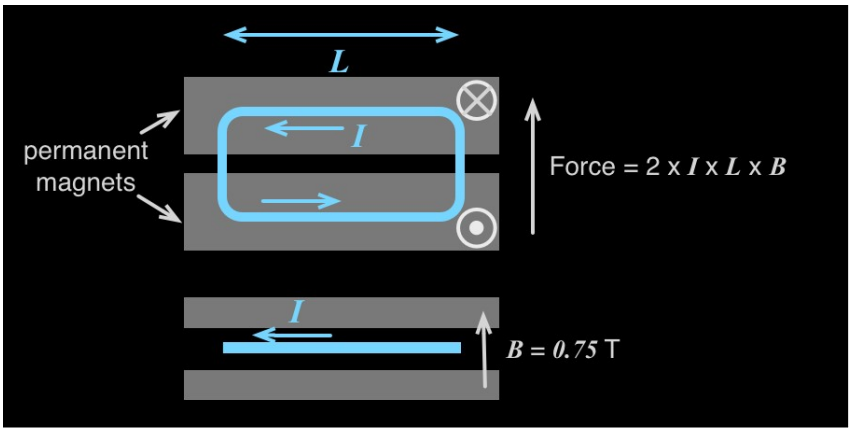

Figure 1.2: Illustration of the physics behind the design of the original Fast Shutter. The top part of this figure illustrates the starting position of the movable coil (blue) with respect to the stationary magnets (grey and labelled at the diagram) as well as the net force the coil experiences when the current pulse is applied. The lower part of the figure shows the top view of the structure and the coil between one of the two pairs of magnets at the top and the bottom. Figure originally included in (Fritschel and Abbott, 2014).

This system uses magnets of opposite polarity to produce the first lifting force in the upward direction that raises the movable coil and mirror payload *as well as* the decelerating force in the downward direction to bring the coil and mirror payload back down to an appropriate spot for sustained blocking of the optical pulse (Fritschel and Abbott, 2014). This particularly novel aspected of the system was patented by LIGO Abbott and Fritschel, 2015.

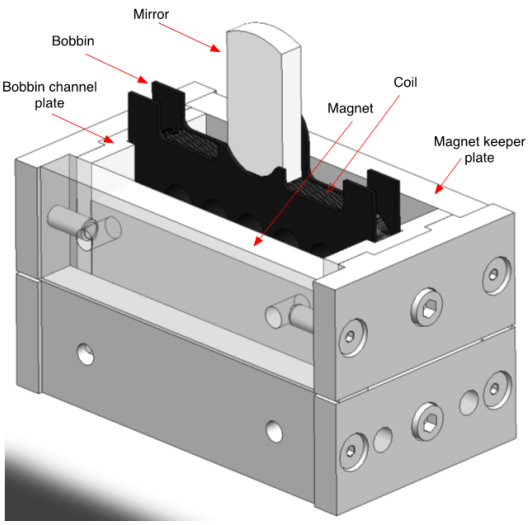

Figure 1.3: Illustration of the physical assembly for the current Fast Shutter system. Figure originally included in (Fritschel and Abbott, 2014).

1.3 Next Generation Fast Shutter System

Introduction

This thesis contains the proposal developed for the next generation shutter along with its characterization and verification of operation. The following sections contain an introduction to the problem as well as a high-level description of the solution designed. Further sections in this thesis contain the equations describing the system's behavior as well as experiments conducted in the lab that informed the design decisions to develop the next generation Fast Shutter system.

Characterization of Problem

While the existing Fast Shutter system is in operation at the LIGO observatories, there is a major drawback to be fixed with the next generation Fast Shutter. The movable coil and mirror payload are lifted by moving wires attached to them and these wires experience a very high acceleration. As a result, these wires have broken several times during operation. Thus, a system without this electo-mechanical

attachment would eliminate this problem. Furthermore, the current pulse necessary to initiate the system should be minimized and there should be a sustained blocking of the optical pulse (i.e. no oscillations in blocking).

Thus, the performance goals for this system include:

- Designing an electromagnetic blocking mechanism that travels upwards $6mm$ in $1ms$ to satisfy time constraints on acceptable length of time exposure of the photodiodes to the optical pulse.
- Minimizing current required for pulse to activate blocking system. More specifically, the voltage applied to the coils would be ideally 500V or lower while satisfying the time and distance specifications.
- Ensuring sustained blocking of optical pulse within the given time constraint (i.e. no oscillatory motion of the mechanism that results in the optical pulse unblocked after the initial blocking/reflecting).

Coil and Payload

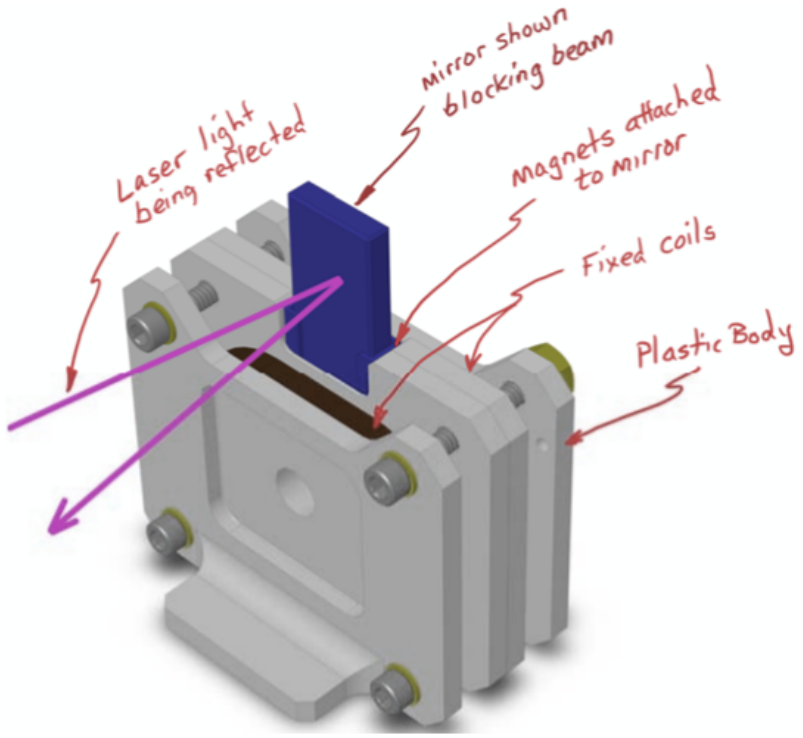

Figure 1.4: Next Generation Fast Shutter System. Figure from (Sanchez, 2016).

Coil Description

In the next generation shutter, there are two coils of approximately 500 turns of 32 AWG copper wire encased in PEEK body. In contrast to the first generation fast shutter system, the coils are stationary in this setup with a moving payload consisting of a mirror to block the optical pulse and magnets.

The coils are connected in parallel. Each coil has an inductance of $4.8mH$ and resistance of 25Ω resulting in a net inductance of $2.4mH$ and net resistance of 12.5Ω.

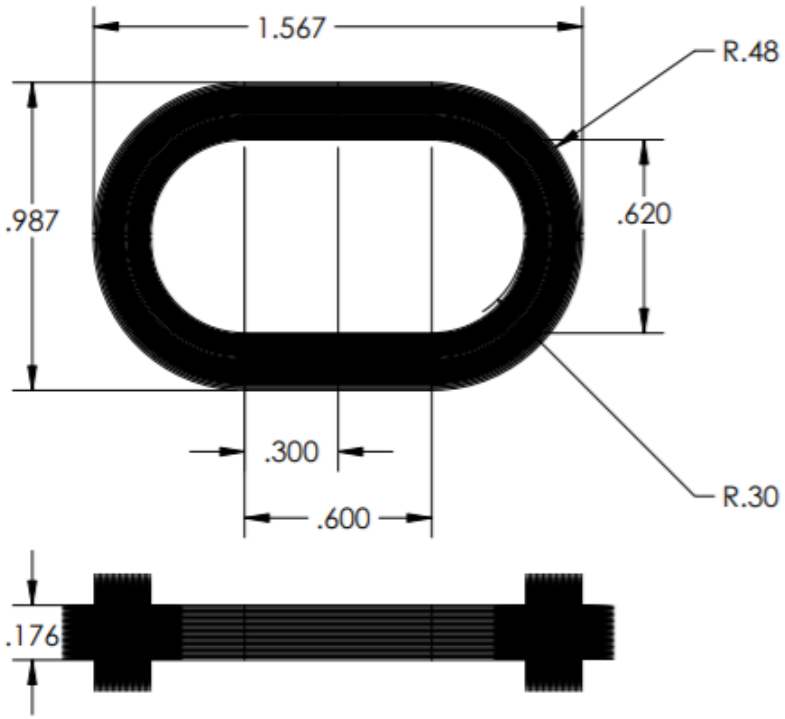

Figure 1.5: Coil Dimensions. Figure from (Sanchez, 2016)

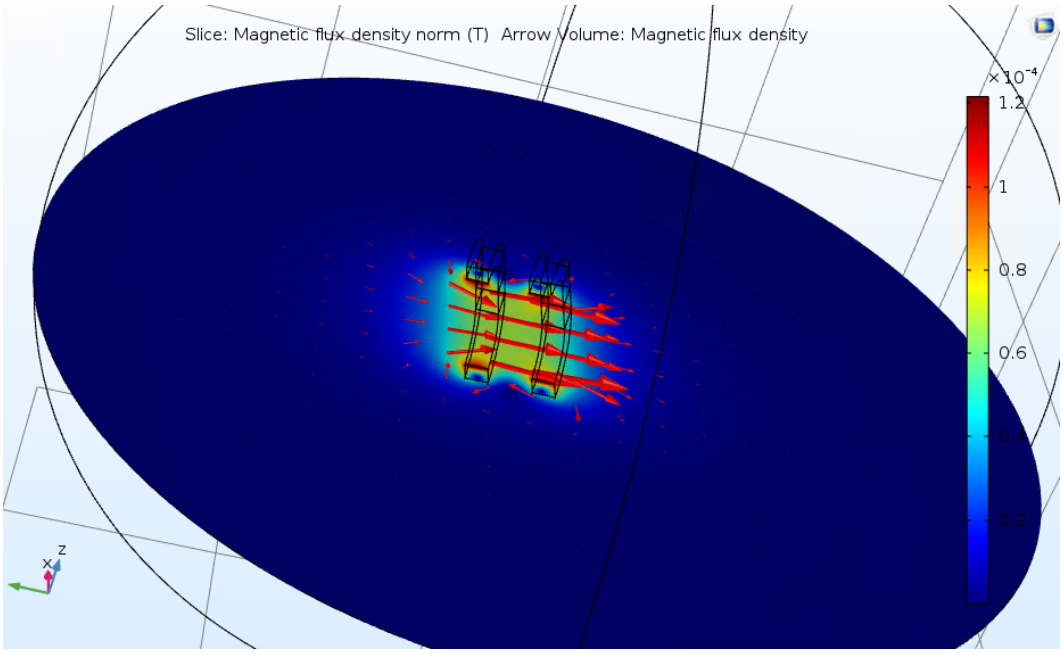

Figure 1.6: Simulation in Comsol of the two coils showing magnetic field and magnetic flux density of the system setup with two coils.

Payload Description

The payload consists of two B842-N52 Neodymium magnets, one at the top of the payload and one at the bottom of payload, held together by two non-magnetic side aluminum rails. A small light mirror flag is attached to the top of the top mirror and blocks the optical pulse.

Figure 1.7: Payload for the next generation Fast Shutter system.

The payload is positioned so that the top and bottom magnets are aligned in the center of the top and bottom horizontal sections of the coils. The optimal vertical position of the magnet between the two coils as well as the optimal separation between the two magnets were characterized and determined.

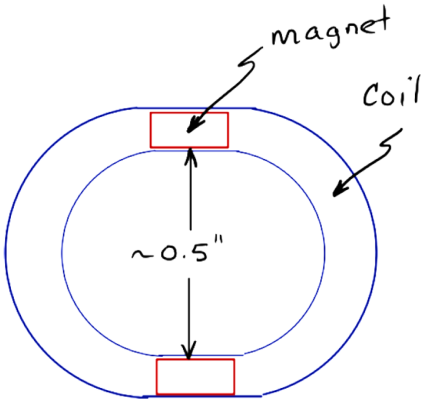

Figure 1.8: Positioning of the magnets with respect to the coil as well as the optimal magnet separation for the payload. Picture from Richard Abbott.

The magnets are polarized in the opposite direction. Since the current is flowing in opposite horizontal directions in the top and bottom horizontal parts of the coils, both magnets will feel a net upward force when a current pulse is applied to the coils connected in series.

When the bottom magnet directly overlaps with the top horizontal part of the coils, the magnet feels a net downward force that brings the payload back down in between the two coils. This electromagnetic force eliminates the need for a mechanical stopping mechanism to bring the payload back down.

Initial Calculations

Assuming constant acceleration, with a distance of $6mm$ to travel in $1ms$ and an initial velocity of $0m/s$, the acceleration was calculated to be $12000m/s^2$.

The current necessary to balance the magnetic force with gravity was found to be $40mA$. From this measurement, the current required for an acceleration of $12000m/s^2$ was calculated to be $49A$.

Copper Eddy Current Damping

The proposed next generation Fast Shutter system utilizes the magnetic force of the coils on two magnets to propel the payload upward, but it has only the force of the coil of one magnet in the other direction to pull the payload back down to a pre-determined resting position to block the optical pulse. As a result, when high current pulses are applied to the extent that the effect of gravity becomes negligible, the next generation Fast Shutter system with just the coils and mirror/magnet payload

is not enough to bring the payload back down to rest between the two coils and block the optical pulse (and the payload flies out of the gap between the two coils).

It is also critical to eliminate any excessive oscillations of the payload once the current pulse is applied. The blocking of the optical pulse should be sustained, with no oscillatory pattern of the payload results in a blocking/unblocking pattern before settling to the sustained blocking position.

To combat both of these issues, the next generation Fast Shutter design utilizes eddy current damping with copper to slow the magnet motion. The characterization of the system without copper damping and various types of copper damping are included.

Next Steps

To completely see this project through completion, a new test prototype has been ordered and is being built. This design will need to be tested in a vacuum chamber to verify its operation in vacuum as all results so far and the design process was conducted in air, with calculations to account for the effect of air resistance and viscous damping. Areas for future work are also identified.

Chapter 2

EXPERIMENTAL SETUP

The test setup consists of a laser, the coils, various payloads, and a photodetector. The laser light reflects off of a mirror to a photodetector serving as an optical gate, with the voltage output recorded by an oscilloscope. An input voltage pulse is applied to the coils to activate the system and causes the payload between the coils jump upward to block the laser light. The difference between the time the voltage pulse was applied and the photodetector detects a reduction in laser light was recorded to b the time it takes to block the light. The current through the coils over time versus when the voltage pulse is applied is measured on an oscilloscope using a Hall Effect current probe.

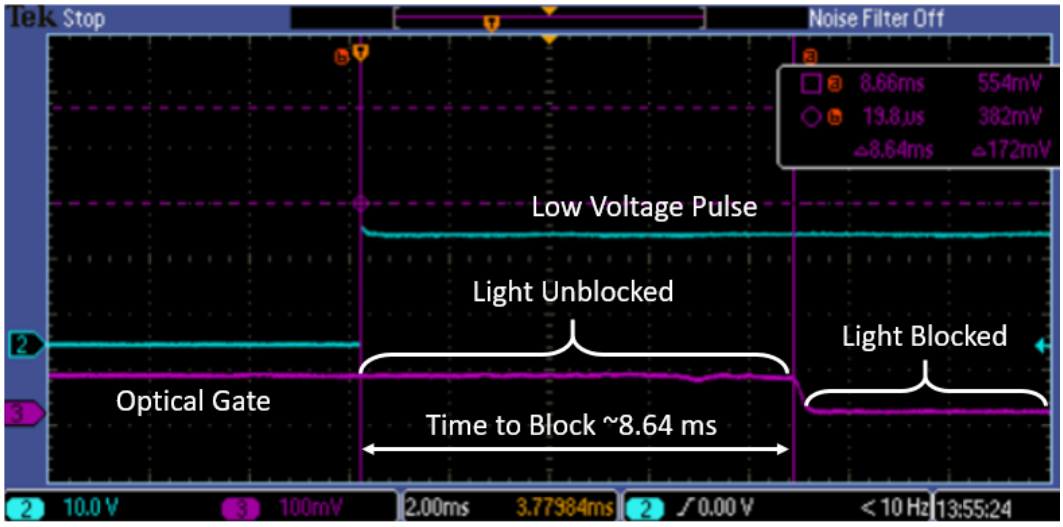

Figure 2.1: Oscilloscope for timing measurement. The voltage applied to the coils (blue) and the photodetector voltage output / optical gate (purple are shown). The cursor on the left indicates when the voltage pulse was applied to the coils. The cursor on the right indicates when the photodetector begins to detect less of the laser light and thus, the laser being blocked. The time difference between the two cursors was recorded as the time for the payload to block the laser light.

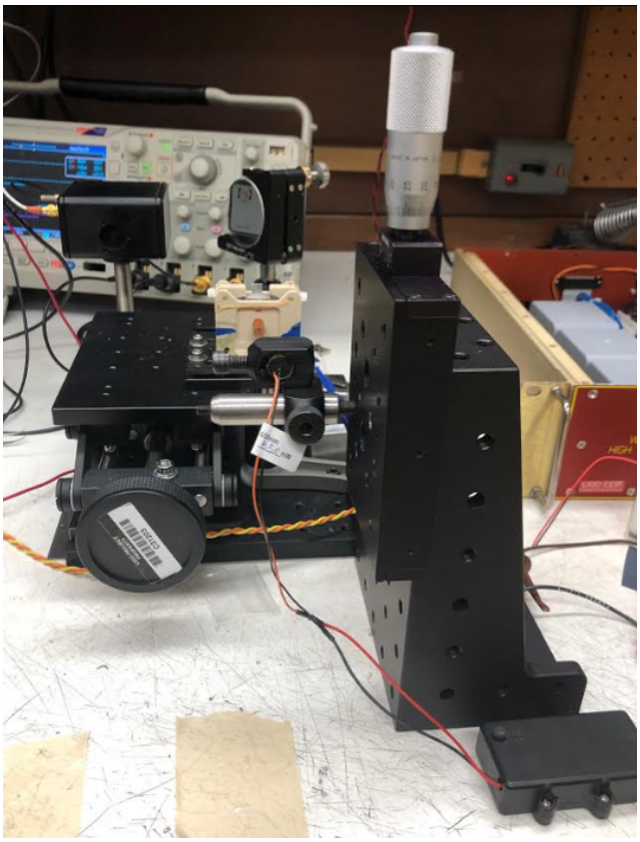

Figure 2.2: Overall test setup for timing measurements.

Figure 2.3: The mirror was set up up to reflect the laser light to the photodetector. With this additional component, the photodetector could be stationary and the mirror used to tune the vertical and horizontal position of the reflection of the laser so that the photodetector could detect the light for various measurements with different payloads and other factors affecting the laser position were changed.

With this setup, the vertical and horizontal position of the laser as well as the vertical

position of the payload between the two coils could be controlled and adjusted for various experiments. The accuracy of the horizontal position was not an important consideration since the vertical blocking is the important aspect of this problem. The vertical positions were measured to the precision of $0.1mm$.

When testing various payloads or sweeps of different parameters for a fixed payload, low voltage experiments were done first up till around 30V before testing with higher voltages that are actually used in the observatories for this system.

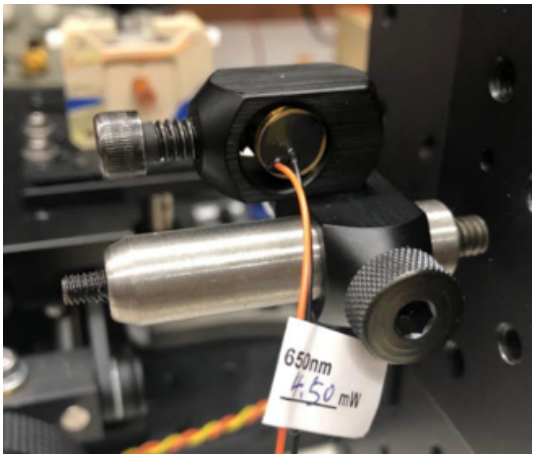

Figure 2.4: A $650nm$ laser used as part of test setup to model the optical pulse used in the LIGO observatories. Both the vertical and horizontal position of the laser could be controlled.

Issues Mitigated with Setup

Data not matching equations

Originally, experimental results did not agree completely with theoretical results due to errors measuring the $6mm$ travel distance consistently from run to run. To mitigate this issue, the laser was mounted on a sliding vertical platform. The height of the laser (the relative distance between the base of the platform and the moving component) is controlled by a micrometer for accurate and repeatable distance measurements. This modification improved the data quality and results in a better fit between theoretical expectations and experimental data.

Ringing voltage

When conducting low voltage measurements, it is critical to directly apply the voltage pulse to the coils from the power supply leads. Using a switch results in the voltage ringing when initially applied due to switch bounce. Using a transistor as a

switch works well, but it has no discernible difference from directly connecting the power supply positive lead to the coils, so the latter approach was used.

Proximity to magnetic surfaces and objects

It is important to ensure no other part of the test setup is magnetic, from the surface the payload rests on to the screws used hold down the PEEK body containing the coils. When magnetic screws were unintentionally used, a damping effect could be observed and the payload was significantly slower, so it is critical that these factors are considered so as not to skew the performance results.

Accurately adjust vertical position of payload

The original test setup was modified to have the coils on an elevated platform that could be moved up and down. The payload is stationary on a rod placed between the coils. The hole for the payload between the coils is open at the top and the bottom. With this setup, the coils can be moved so that the starting vertical position of the payload with respect to the coils can be adjusted. A caliper was used for these measurements, with an accuracy up to $0.001in$.

Friction between payload and coils structure

The gap for the payload has little play, so there is no leeway for any extra spacing between the roads, mirror, and magnet(s) when the parts of the payload were glued together. Any error in constructing the payloads will cause unintentional damping effects due to the friction between the PEEK body containing the coils and the payload.

Heating magnets

To quickly assemble and disassemble payloads, which was necessary to be able to use the side rails (which were limited in number) to hold the payload and magnet(s) together, a heat gun was used to remove the epoxy applied to construct the payload. The temperature necessary to melt the epoxy approached the Curie temperature of the magnets, resulting in significantly weaker magnet surface fields. Thus, it is important to measure the surface field of the magnets used to construct different payloads so that the magnetic fields are comparable between payloads.

Air damping

The bottom of the channel guiding the payload was left mostly open (the payload was held upright in between the coils using a rod underneath) instead of closing it and letting the payload rest on the bottom to minimize any air damping effects. This would not be a problem in the final system which is in vacuum, but this adjustment was made so that our experimental results would more closely translate to what would happen in the observatories.

Simulations

This system was partially simulated in Ansys Maxwell and Comsol. Adding in factors that completely and accurately described the system proved to be time-consuming, so experiments at low voltages were used to inform tests at high voltages and analytical equations were used to explore additional theories.

Balanced payload

If the payload is not wide enough in the z direction (in and out with respect to the plane of the coil), it can be slightly tilted before a pulse is applied since the payload is balanced on a rod. This issue is easily solved by using the aluminum side rails to hold the magnet(s) and mirror together. That way, the "depth" was consistently set and perfectly fitted for the gap the payload fit in between the two coils.

Chapter 3

PAYLOAD

A variety of payloads were characterized to determine their performance and feasibility of use in the final proposed system given the time specification. This section covers timing results for the payloads tested along with observations on the optimal payload.

There were two different models for the mirror used when constructing the different payloads. The first model used was an aluminum block weighing $3.4g$ while the second was a much lighter "flag" model weighing $0.15g$. The payload numbers assigned below are used to refer to the various payloads throughout.

Several different magnet sizes and shapes were considered, but the choices were quickly narrowed down to two magnets:

Magnet	Dimensions (in)	Weight (g)	Surface Field (Gauss)
B882G-N52	$\frac{1}{2}$ x $\frac{1}{2}$ x $\frac{1}{8}$	3.84	3032
B842-N52	$\frac{1}{2}$ x $\frac{1}{4}$ x $\frac{1}{8}$	1.92	4174

Table 3.1: Primary magnets considered for payload.

The material for both magnets was neodymium (NdFeB), grade 52. The grade indicates the highest strength these magnets can be magnetized to, so grade 52 was chosen as it is the highest grade of NdFeB magnets commercially available. NdFeB magnets themselves were chosen because they are one of the strongest magnets that can be purchased. The magnetization direction was "thru thickness" as necessary for the magnets to be oriented in the payload as shown and feel an upwards force due to the magnetic field of the coils. The maximum operating temperature for both these magnets is 176 ° F, which was important to be mindful of when assembling various payloads as noted above in the experimental setup chapter.

Payload Number	Mass (g)	Magnet
1	8.0	1 B882G-N52 Magnet
2	6.0	1 B842-N52 Magnet

Table 3.2: Descriptions of payloads with aluminum block mirror model.

Payload Number	Mass (g)	Number of Magnets	Magnet Spacing (in)
3	2.9	1	N/A
4	4.7	2	0.5
5	4.5	2	0.4
6	4.45	2	0.3
7	4.4	2	0.2

Table 3.3: Description of payloads with flag mirror model. All magnets for these payloads are B842-N52 magnets. Magnet spacing refers to the distance between the bottom edge of the top magnet and the top edge of the bottom magnet.

Figure 3.1: Pictures of Payloads 1 through 7.

For constant acceleration a, $t \propto a^{-0.5}$ for time duration t. Since $a \propto F_B$ for magnetic force F_B and current and voltage are proportional to the magnetic force, we would expect $t \propto V^{-0.5}$ for voltage V, regardless of payload tested. This relation may not always strictly hold because it assumes constant acceleration while the payload is accelerating throughout its $6mm$ travel (as shown later). In our results, however, we see this relation does hold for all payloads tested except for Payload 1. The measurements for Payload 1 were done with a less robust test setup, however, which likely resulted in measurement errors contributing to the slight deviation between the expected relation and what was observed.

Below are the results for various payloads and the time it took for them to travel a $6mm$ distance to block a laser light at low voltages ($10V$ to $30V$). Exponential fits from this data were used to extrapolate to higher voltages and the voltage necessary

for $1ms$ travel, so that the most promising payload could then be further tested and verified at higher voltages.

3.1 Payload 1: B882G-N52 Magnet + Aluminum Block

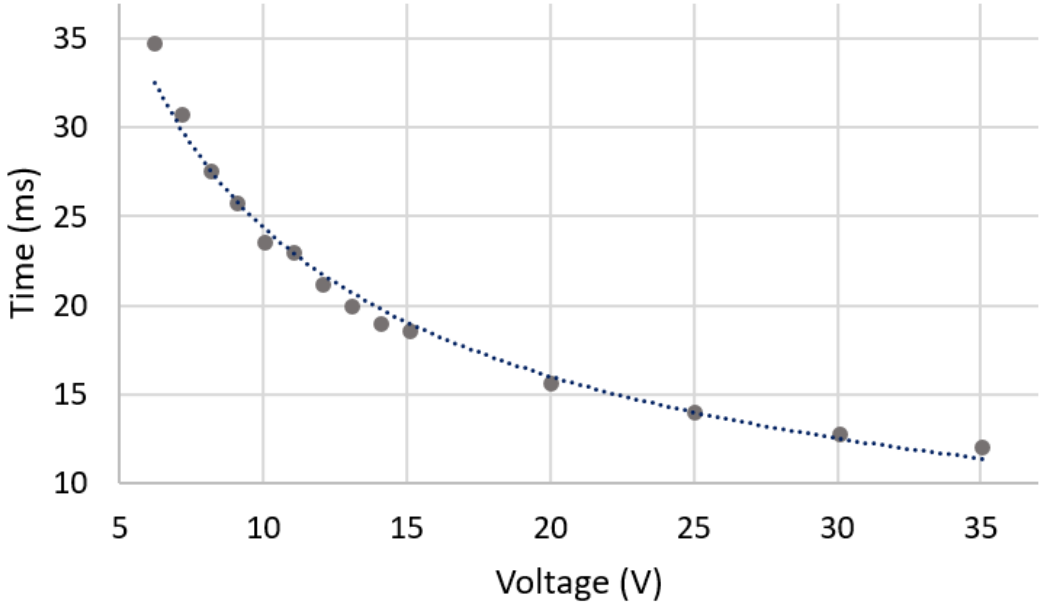

Figure 3.2: Time to travel 6mm for Payload 1 at various low voltages applied to coils with exponential fit.

The exponential fit for this payload was:

$$t = 98.725 * v^{-0.607}$$
$$\text{with } R^2 = 0.9893$$

For this payload, $t \propto v^{-0.6}$ (with a high R^2 indicative of a good fit), which is slightly different from the relation justified above. This discrepancy can be attributed to the use of the earlier setup which could have contributed to possible inconsistencies when taking measurements as we see this relation holds for the final test setup and all the other measurements recorded.

With this previous setup, Payload 2 was always at least 14% faster than Payload 1, indicating that the extra $\frac{1}{4}$ in in height gained with the taller magnet in Payload 1 was not affected enough by the magnetic field of the coils to overcome the extra gravitational force on the payload due to the two extra grams. The height of the bottom part of the coil is $0.1835in$, so it makes sense that the shorter magnet (height

$0.25in$) has a better performance because it has a greater overlap with the coil than the taller magnet (height $0.50in$) when starting out and the overall payload with the smaller magnet weighs less.

In addition, in this payload, the magnet was $\frac{3.84g}{8.0g} * 100 = 48\%$ the mass of the entire payload. Once the magnet became the majority of the mass of the payload, any net effect from the magnetic force on it accelerating the payload upwards was cancelled by a proportional gravitational force downwards on it from the extra mass. Thus, payloads with less mass and in particular, payloads where the magnet was not the dominant source of mass were considered.

Due to these observations, Payload 1 was determined to not be an optimal solution. However, it was useful to conduct this experiment to verify that the general concept of this system with stationary coils and a moving magnet and mirror payload. This experiment also showed that a more robust test setup needed to be built to understand the behavior of other payloads considered.

3.2 Payload 2: B842-N52 Magnet + Aluminum Block

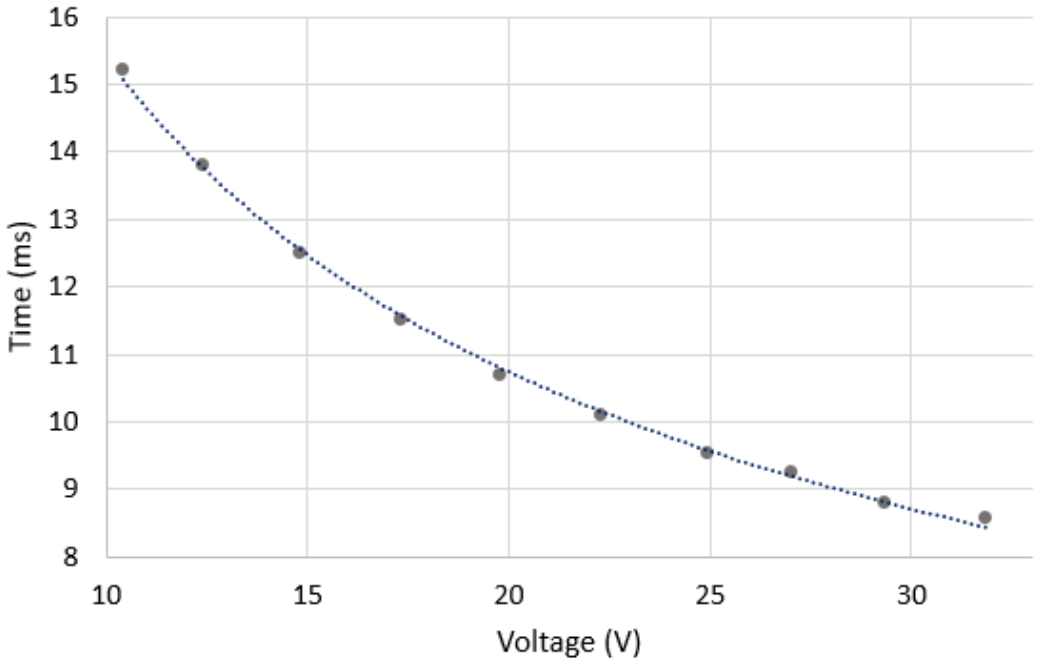

Figure 3.3: Time to travel 6mm for Payload 2 at various low voltages applied to coils with exponential fit.

The exponential fit for this payload was:

$$t = 50.64 * v^{-0.518}$$
$$\text{with } R^2 = 0.9984$$
$$\text{Projected voltage necessary for } 1ms \text{ travel: } 1952V$$

The exponential fit for this system is much closer to $t \propto v^{-0.5}$, so a few more modifications were made to the setup, particularly with measuring $6mm$ with an accuracy of up to $0.1mm$ so that the time measurements were consistent from run to run for future payloads tested.

The projected voltage for this payload was 4 times the ideal amount specified, so this solution would not be feasible for the system. This payload had a lot of unnecessary mass however, since a significant portion of the aluminum block neither helped with upward travel (like the magnet) nor blocked the laser (like the top part of the aluminum block), so a payload with reduced mass was next explored.

3.3 Payload 3: B842-N52 Magnet + Flag

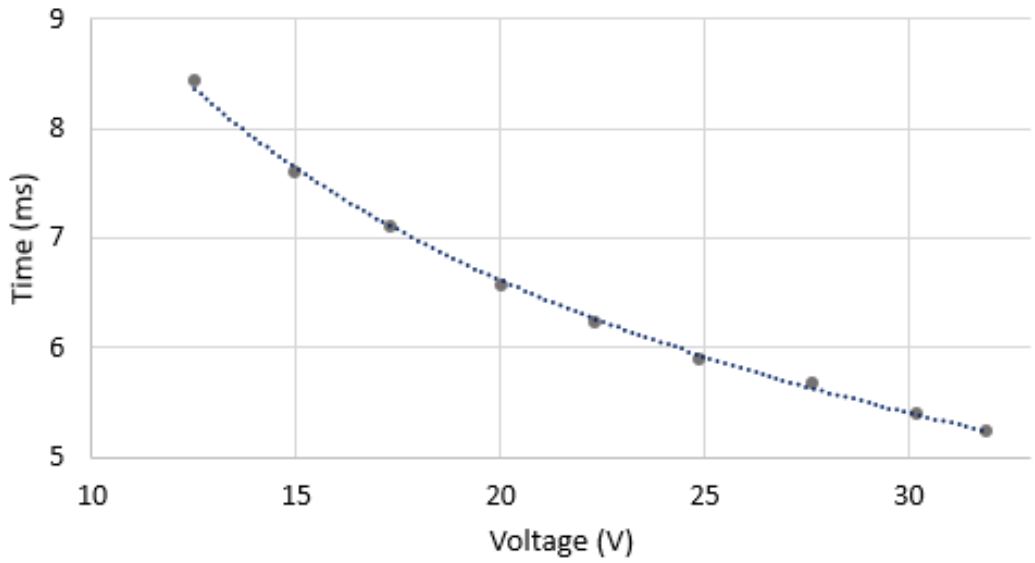

Figure 3.4: Time to travel 6mm for Payload 3 at various low voltages applied to coils with exponential fit.

The exponential fit for this payload was:

$$t = 29.564 * v^{-0.5}$$
$$\text{with } R^2 = 0.9985$$
$$\text{Projected voltage necessary for } 1ms \text{ travel: } 870V$$

Projected voltage necessary for $1.9ms$ travel: $242V$

This exponential fit completely agreed with our theoretical expectation of $t = v^{-0.5}$, lending more credibility to the experimental setup and data. This test setup also yielded similar fits for various other payloads and became the final setup used and described.

If the mass of the payload is reduced by a factor of n, the acceleration increases by a factor of n, resulting in a decrease in time by a factor of $\sqrt{n}$. Since $t \propto V^{-0.5}$, the new voltage required for the payload to satisfy the same distance and time criteria is then reduced by a factor of n. Thus, reducing the mass of the payload should directly correspond to a reduction in the voltage necessary for $1ms$ travel.

The mass ratio of Payload 2 to Payload 3 is $\frac{6.0g}{2.9g} = 2.1$. The ratio of the expected voltage necessary for $1ms$ travel, based on their exponential fits is $\frac{1952V}{870V} = 2.2$, which is within a 5% error since we would expect both these ratios to be equal. Our experimental data thus agrees with what we would expect in a situation with constant acceleration.

Payload 3 was significantly more promising than both Payload 1 and Payload 2 because the extrapolation to voltage required for $1ms$ travel was under 1000V and closer to 500V as desired in the specifications. LIGO currently operates the fast shutter at around $250V$ for a $1.9ms$ travel time, so this design would be on par with the current setup with the added benefit of a stationary coil and no moving wires. From this point forward, the goal was to minimize the voltage required to activate the system while not sacrificing this time performance.

3.4 Payload 4: 2 B842-N52 Magnets + Flag

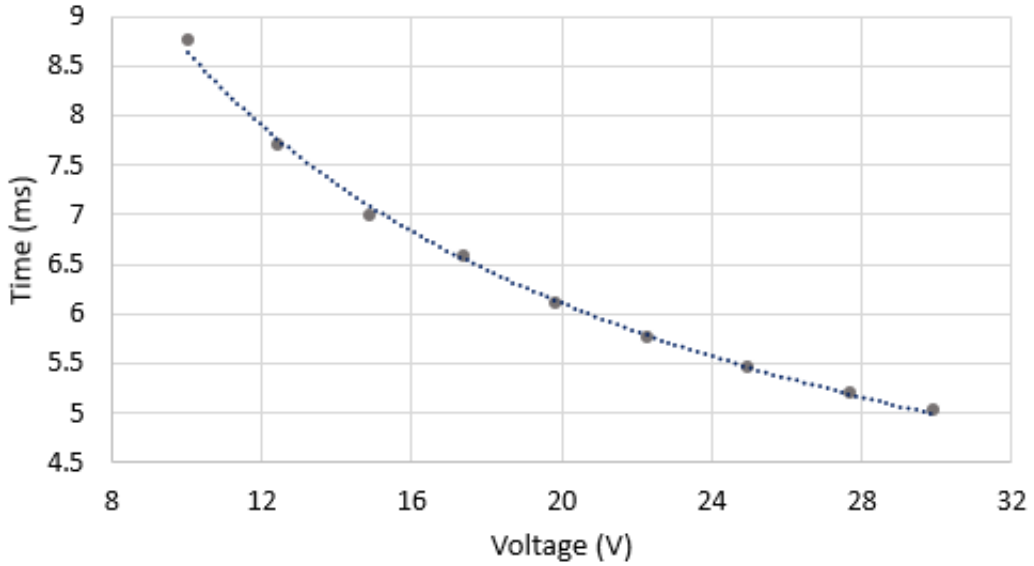

Figure 3.5: Time to travel 6mm for Payload 4 at various low voltages applied to coils with exponential fit.

The exponential fit for this payload was:

$$t = 27.523 * v^{-0.502}$$

with $R^2 = 0.9981$

Projected voltage necessary for $1ms$ travel: $738V$

Projected voltage necessary for $1.9ms$ travel: $205V$

Projected time with 500V applied: $1.22ms$

For all the previous payloads, the bottom of the coil windings was used to propel the payload forward and then the top of the coil windings was used to bring the magnet back down. However, the top of the coil windings generate a magnetic field that could be utilized to the system's advantage at the beginning to satisfy the time specification, so using two magnets as part of the payload was explored. While this approach would add more mass to the system, it would also double the magnetic force on the payload if the top magnet was flipped with the opposite magnetic orientation. Since the current through the coil flows in the opposite direction of the current through the bottom of the coil since the coil is a loop, the force on the top magnet would be upwards as well, generating twice the force to accelerate the payload upwards.

At low voltages, the gravitational force was not negligible compared to the magnetic force as observed at high voltages, so the effect of the extra mass diminished the effect of doubling the magnetic force at the beginning.

The use of two magnets instead of one results in twice the force contributing to the initial acceleration. Since $t \propto F^{-0.5}$ for time t and force F, Payload 4 should travel a fixed distance in $\frac{1}{\sqrt{2}}$ of the time compared to the time taken by Payload 3.

The projected voltage necessary for $1ms$ travel for Payload 3 was $870V$, so plugging in that voltage in the exponential fit should give $\frac{1}{\sqrt{2}} * 1ms = 0.707ms$. In reality, the exponential fit gives $t = 0.921ms$, which is a slower result than expected. However, this discrepancy can be attributed to the fact that while voltage and distance are kept constant, the mass is significantly different between the two payloads. The extra $2g$ of mass from Payload 4 contributes to a stronger gravitational force opposing the dual magnetic forces at the start, resulting in the upward travel taking longer than our expectation. This effect will also be more prominent at low voltages when the gravitational force is still on par with the magnetic force strength.

Experiments to determine the optimal spacing between the payload magnets are detailed in a separate chapter. The spacing affects the magnetic force on both magnets and the resulting acceleration of the payload.

This payload came the closest to satisfying the $500V$ requirement for $1ms$ travel and requires less than half of that voltage for $1.9ms$ travel which is LIGO's current operating time. Furthermore, with $500V$, this payload's exponential load predicts the $6mm$ can be traveled in $1.2ms$ which is very close to half the current operating time in the observatories. As a result, this payload was tested at higher voltages to see whether it behaved the same and would be a feasible approach for the next generation shutter system.

Chapter 4

SWEETSPOT WITHIN COIL

The vertical starting position of the payload between the two coils dramatically changed the effect of the magnetic force (to the extent that starting at a non-optimal position could result in the payload not moving at all). To determine the optimal "sweetspot", the voltage was set to a constant $15V$, and the time for a payload to travel $6mm$ was measured as a function of the payload vertical starting position. The scale is with respect to the base of the table the setup is on, so a constant scale factor can be applied to the x-axis of the graph below to get the starting position of the payload relative to the coils. The sweetspot was experimentally measured for Payload 2 and Payload 3 which have one magnet, so that one magnet's optimal position could be independently determined before looking at a two magnet payload.

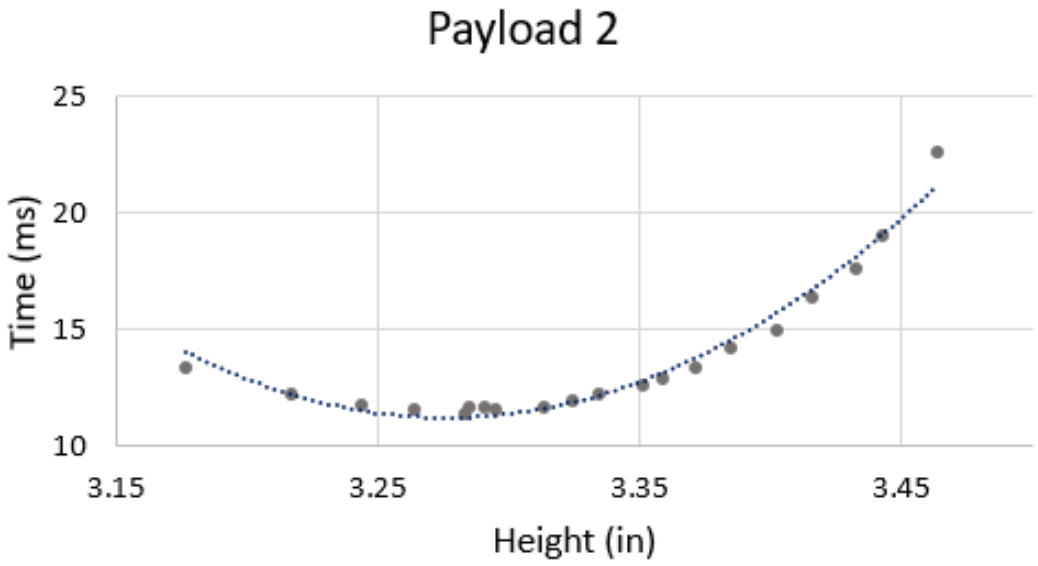

Figure 4.1: Time (ms) to travel $6mm$ at $15V$ for various starting positions of Payload 2 within the two coils.

The fit for this data was:

$$t = 283.17h^2 - 1855.6h + 3051.1$$

where t indicates time, h indicates height

with $R^2 = 0.9744$

Minimum based on experiment: $11.4ms$ corresponding to $3.283in$

Minimum based on fit: $3.28in$

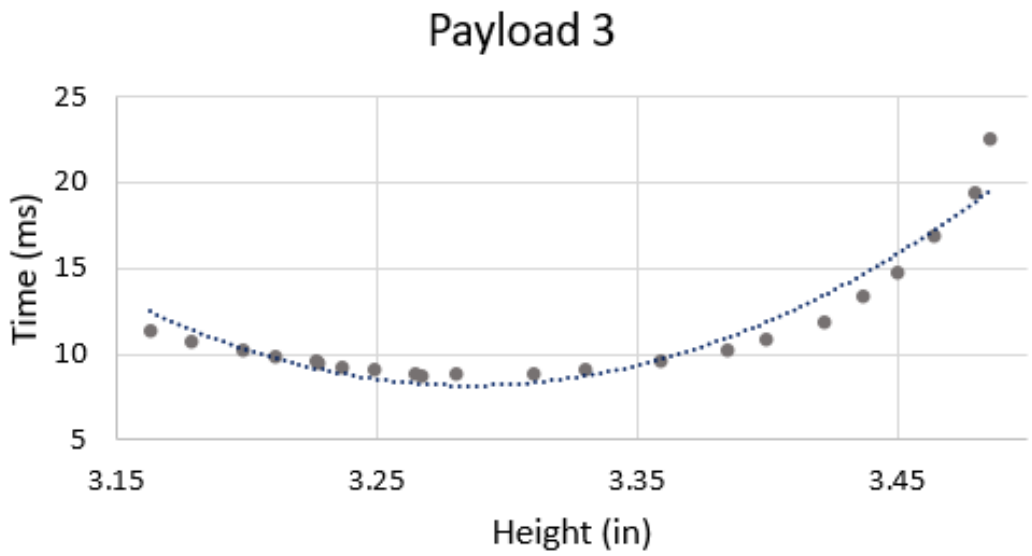

Figure 4.2: Time (ms) to travel $6mm$ at $15V$ for various starting positions of Payload 3 within the two coils.

The fit for this data was:

$$t = 284.24h^2 - 1867.9h + 3077$$

where t indicates time, h indicates height

with $R^2 = 0.9314$

Minimum based on experiment: $8.76ms$ corresponding to $3.267in$

Minimum based on fit: $3.28in$

The fits for both Payload 2 and Payload 3 are very similar and both fits give the optimal sweetspot as starting the bottom of the payload at $3.28in$. The magnet affected by the magnetic force of the coils is the same between the two payloads and is oriented the same way with just a different mass of non-magnetic material glued above it, so it is expected that both payloads yield the same sweetspot position.

The sweetspot for one magnet should be in a position of optimal coupling between the magnet and the bottom coil. The height of the magnet is $0.25in$ while the height of the bottom coils is $0.1835in$, so they are very close in height. The $3.28in$ found from the experimental data and fits corresponds to the payload starting at the bottom of the coil (this is vertically offset from the PEEK body shown in the pictures of the

setup as the coil starts a bit above the bottom of the PEEK body encasing), which agrees with what is expected.

Chapter 5

OPTIMAL SPACING BETWEEN MAGNETS

A similar sweetspot analysis was conducted for Payloads 4, 5, 6, and 7 which all have two magnets and the flag mirror block as part of the payload. It was expected that the sweetspot would be when the magnets were spaced such that the direct overlap between the bottom magnet and the bottom part of the coil as well as the top magnet and the top part of the coil were maximized as this had also been verified experimentally with the one bottom magnet case.

The distance between the bottom of the top coil and the top of the bottom coil is $0.620in$, while the distance between the top of the bottom of the coil and the bottom of the bottom coil is $0.987in$, as shown in the picture of coil dimensions figure. The height of both magnets is $0.25in$, so the total height of the magnets is $0.25in * 2 = 0.5in$. Thus, the optimal distance between the two magnets should be $0.987in - 0.5in = 0.487in$.

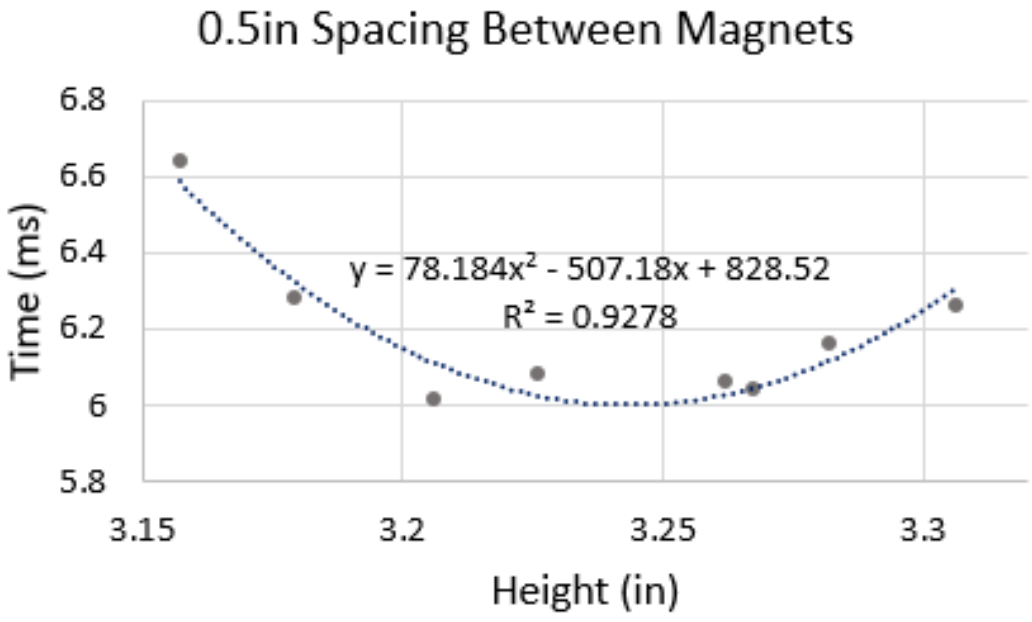

Figure 5.1: Time (ms) to travel $6mm$ at $20V$ for various starting positions of Payload 4 within the two coils.

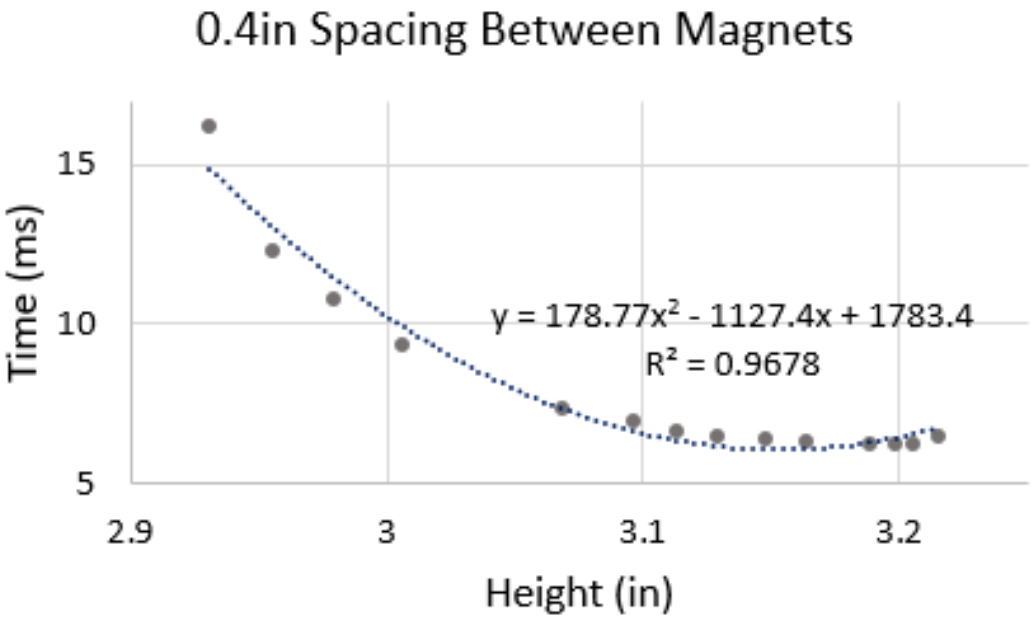

Figure 5.2: Time (ms) to travel 6*mm* at 20*V* for various starting positions of Payload 5 within the two coils.

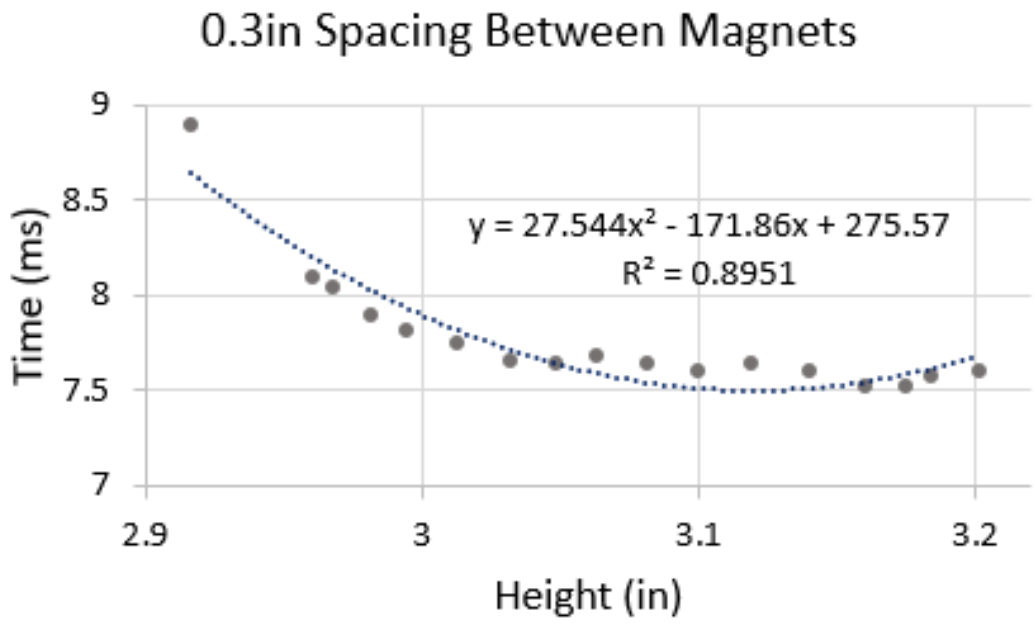

Figure 5.3: Time (ms) to travel 6*mm* at 20*V* for various starting positions of Payload 6 within the two coils.

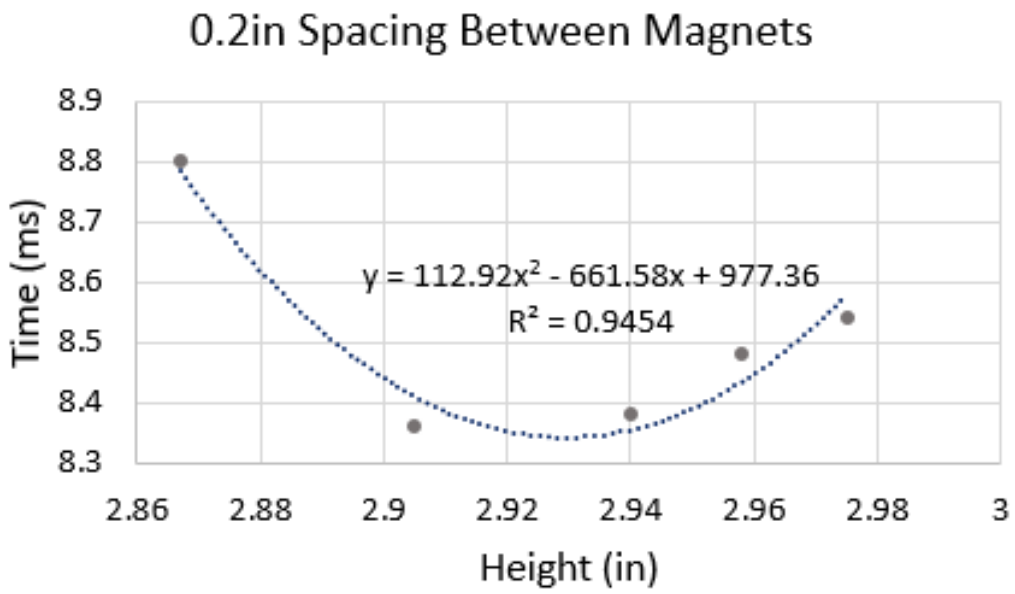

Figure 5.4: Time (ms) to travel $6mm$ at $20V$ for various starting positions of Payload 7 within the two coils.

Payload 4 had previously been characterized with varying low voltages, so that data was also used to inform this decision. It was also clear that Payload 7 was significantly slower compared to rest of the payloads, so less data points were measured. This was expected as with a $0.2in$ spacing and the bottom of the bottom magnet aligned with the bottom of the bottom coil, the top of the top magnet was $0.25in$ (height of bottom magnet) + $0.2in$ (spacing) + $0.25in$ (height of top magnet) = $0.7in$ from the bottom of the coil whereas the bottom of the top coil is $0.8035in$ ($0.987in$ [distance between the top of the top coil and bottom of the bottom coil] - $0.1835in$ [height of top coil]) from the same reference point. Thus, the top magnet starts with no direct overlap with the top coil and directly overlaps with the top part of the coil for only half its travel ($0.15in$). Thus, it unsurprising that Payload 7 does not perform as well as the other payloads since its upward acceleration is not as affected by the addition of the top magnet.

As can be seen from these sweetspot experiments for payloads with various magnet spacing, the $0.5in$ spacing performed the best and that also agrees with our intuition. As a result, the optimal spacing for the magnets in a two magnet payload was determined to be $0.5in$.

Chapter 6

HIGH VOLTAGE

The system is driven with high voltages through large charging and discharging capacitors in a fast shutter driver system previously built. This driver contains a programmable system-on-chip (Cypress Semiconductor PSoC 3) that can be programmed to output a high voltage pulse for a specified amount of time. A few modifications were made to the original circuitry to allow for pulses longer than $10ms$ when testing.

If the voltage is turned off before the bottom magnet reaches the top of the coil, then there is no magnetic force downward on the magnet pushing the payload back down into guiding channel between the coils, so it is critical the timing is correctly set so the payload does not go flying. It is also important to note that the inductance of the coil results in a $1ms$ rise time for the current.

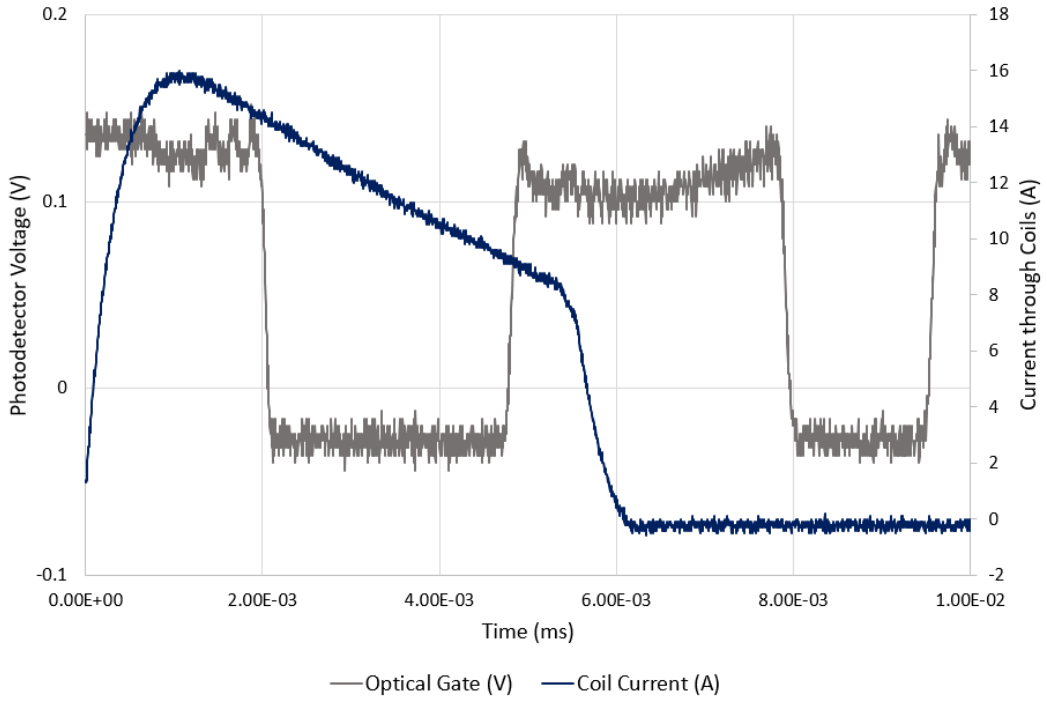

Figure 6.1: Photodetector voltage (grey) and current through coils (blue) over time when high voltage pulse ($240V$ in this particular case) is applied to the coils. The voltage pulse from the fast shutter driving circuit was turned off around 5ms for this graph.

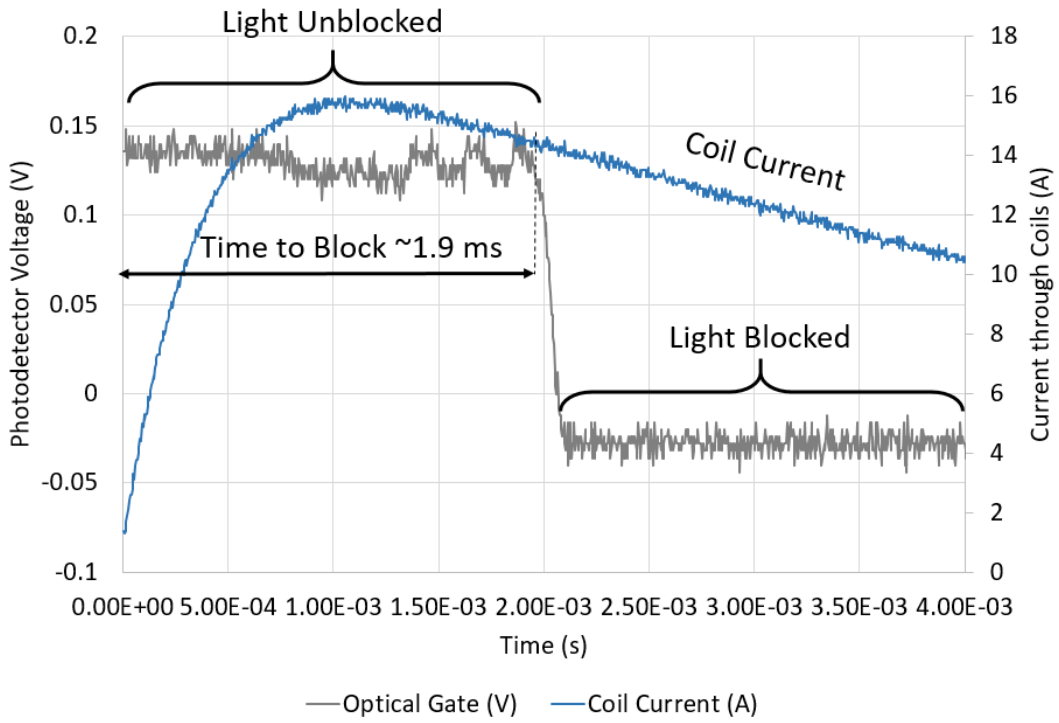

Figure 6.2: Current through the coils and optical gate laser light detection for a $240V$ pulse. The optical gate indicates when the light has been blocked and reflected by the fast shutter system. This system satisfies the specifications of the old system: with the $240V$ pulse that is used with the previous fast shutter, the payload is able to travel $6mm$ in $1.9ms$ and block an optical pulse as is currently done.

When tested with Payload 4 at around $240V$, the light was blocked at $1.9ms$, with the slight deviation from our exponential fit at low voltages likely explained by small measurement errors. These numbers are still reasonable given our specifications and LIGO's current operating conditions. When the light is blocked, the bottom magnet (as well as rest of the payload) has moved up $6mm = 0.24in$. The height of the bottom coil is $0.1835in$ as shown earlier, so the bottom magnet is now past the main interaction region with the coil as there is no direct overlap between the magnet and coil. This point corresponds to the first drop in voltage detected by the photodetector.

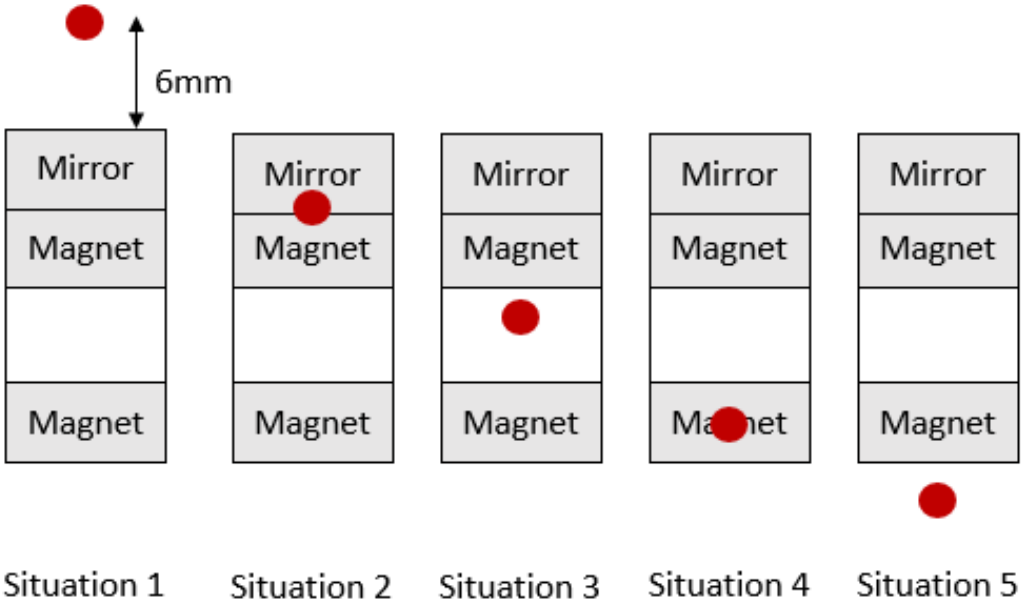

Figure 6.3: Possible situations for the relation between the location of the payload with respect to the stationary laser light. Situation 1: Initial starting position below voltage pulse is applied. Laser light is 6*mm* above the top of the payload. Situation 2: The mirror and/top magnet are blocking the laser light. Situation 3: The laser light is not being blocked and is shining through the gap between the magnets part of the payload. Situation 4: The bottom magnet is blocking the laser light. Situation 5: The laser light is not being blocked as the entire payload is above the laser light position.

In this particular example, the voltage pulse was not applied for long enough and the payload went flying. Thus, the first sustained blocking of the laser light (low photodetector voltage on the graph from around 2*ms* to 5*ms* corresponds to the time when the laser light was blocked by the payload and then the top magnet as the payload kept traveling upward (Situation 2). The detection of the light again from 5*ms* to 8*ms* corresponds to the time when the laser light was shining through the gap in the payload between the two magnets (Situation 3) and then the laser light is blocked again around 8*ms* as the top of bottom magnet reaches the laser light (Situation 4). Then, at around 10*ms*, the photodetector begins detecting the laser light again indicating that the bottom of the bottom magnet is now 6*mm* above where the top of the payload started and the payload is completely out of the hole (Situation 5).

Thus, by the time the voltage pulse is turned off at 5*ms*, the bottom magnet is still in the area between the two coils and has no direct overlap with the top coil yet. When

the bottom magnet directly overlaps with the top coil, there is no voltage pulse being applied and the current through the coils is $0A$ as can be seen on the graph. As a result, there is no magnetic force applied on the bottom magnet that brings the whole payload back down into the hole. At $10ms$ however, the bottom magnet is past the top coil, so if the voltage pulse was turned off then, there would be a magnetic force on the bottom magnet in the downward direction.

When the pulse was extended to $10ms$ however, the payload still flew out of the hole because the initial upward travel was due to the magnetic force on two magnets, but the intended restoring force was only due to the magnetic force on the bottom magnet as the top magnet was not near a coil. The downward magnetic force was not sufficient to bring down a payload that had been accelerated up with twice that force upward initially.

6.1 Comparison with Low Voltage Behavior

Since the payload was brought back down in the hole between the coils at low voltages, the current through the coil was measured for a lower voltage to observe the system's behavior.

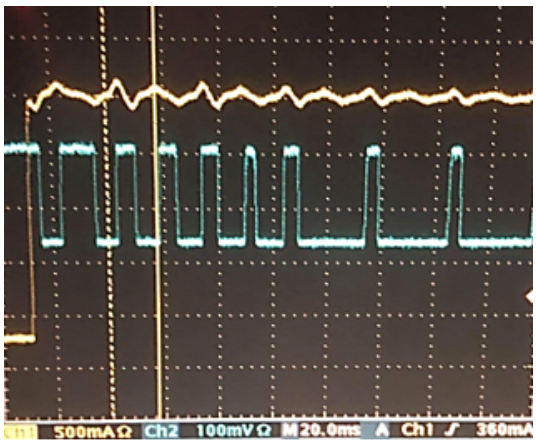

Figure 6.4: Photodetector voltage (blue) and current through coils (yellow) over time when low voltage ($32V$) is applied to the coils. The voltage pulse was applied for a time significantly longer than 10ms.

The photodetector voltage displays oscillations in the blocking of the laser light for two different reasons:

1. the payload is so high that the bottom of the top magnet is above $6mm$, so the laser light is detected by the photodetector through the gap between the two

magnets in the payload

2. the top of the flag mirror model part of the payload has fallen below 6*mm*, so there is nothing blocking the laser light any longer

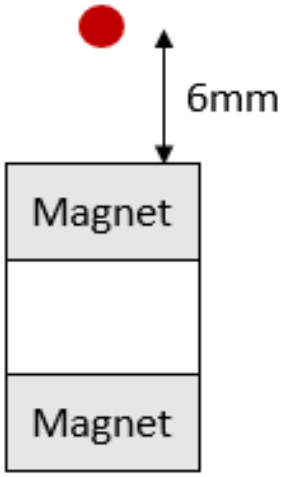

Figure 6.5: Initial setup of the payload with respect to the laser light before voltage pulse is applied.

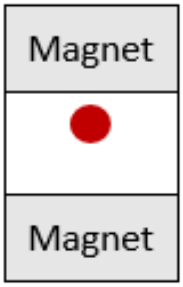

Figure 6.6: Oscillation type 1, where the laser light is detected by the optical gate because it is shining through the gap between the magnets part of Payload 4.

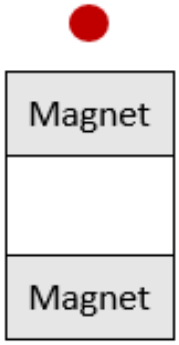

Figure 6.7: Oscillation type 2, where the laser light is detected by the optical gate because the entire payload has fallen below the height of the laser (6*mm* in this experiment).

The first, third, and fifth "laser light unblocked" sections in the photodetector voltage correspond to the first reason, with varying widths because the payload's oscillation height decreases over time after the initial voltage pulse.

While the first type of oscillation needs to be completely eliminated, the second type of oscillation only needs to be minimized to the extent that there is no unblocking of the optical pulse once it has been blocked. This minimization can be achieved well with copper damping as described later.

The oscillations when the entire payload falls below the "block point" are periodic. They also correspond to an increase peak in current from the back EMF generated by the bottom magnet directly overlapping with the top coil. Since this increase in current was present at low voltages and in the first generation fast shutter system, it became evident that the only variable that had changed was the presence of two magnets contributing to the upward force but only one magnet contributing to the downward force. At low voltages, the two magnet payload was brought back down because the force of gravity was still significant in comparison to the downward magnetic force on the bottom magnet once the payload was in the air so the forces added together.

6.2 Comparison with Existing Fast Shutter

Energy Balance Difference

The existing fast shutter utilizes magnetic damping to bring the payload back down into the guiding channel after the initial upward acceleration. At the start, the moving coil is halfway between both magnets. The bottom and top parts of the

coil feels an upward and downward force from the magnetic field of the bottom and top magnets, respectively, since the current is flowing in different directions in both parts of the coil and the magnets are oppositely polarized. From an energy standpoint, this results in $2 * F * \frac{1}{2} * d = F * d$, where F is the magnetic force due to one magnet and d is the height of one magnet. For the initial acceleration, the bottom coil travels a distance $\frac{1}{2} * d$ overlapping with the bottom magnet as does the top coil with the top magnet.

When coming back down, the top part of the coil is no longer in the interaction region with the top magnet, while the bottom part of the coil is. This results in a downward force on the coil due to the magnet. Since the coil is completely overlapping with the top magnet, the energy in this situation is $F * d$, since F is still the magnetic force due to one magnet and d is the height of the top magnet. Thus, both the upward and downward movement situations have the same energy, so there is never a situation where the forces and energy are unbalanced and the payload goes flying.

In contrast, the new proposal with two magnets as part of the moving payload (Payload 4) does not benefit from a similar equitable design. At the start, there are two magnets directly overlapping with the top and bottom parts of the stationary coils, but at the end, there is only one magnet directly overlapping with the top part of the coils. As a result, the force attempting to bring the payload back down into the guiding channel between the coils is half as strong as the force resulting in the initial acceleration. Thus, at high voltages when gravity becomes negligible compared to the magnetic force, the payload goes flying and does not come back down.

Back EMF

In the graph of current through the coils with the proposed design, there is no increase in the current indicating any back EMF behavior. The existing shutter design did have a significant back EMF current present due to the sustained overlap between the magnets and the coil as the coil vertically moved. In the proposed design, however, the magnet has no direct overlap with the coil windings once the payload has accelerated upward to block the optical pulse as the magnets are much smaller compared to the existing case and only $0.25in$ tall. Since the magnet travels $6mm = 0.24in$ to block the optical pulse, the magnet and bottom coils windings have no direct overlap once the payload is blocking the pulse as the height of the windings of the bottom coil is $0.1835in$. Thus, the back EMF is negligible in this situation.

Chapter 7

EDDY CURRENT DAMPING WITH COPPER

Eddy current damping with copper was explored in order to

- minimize the oscillation of the payload that results in the laser shining through after being blocked once
- provide the necessary force to bring the payload back down for payloads with two magnets where both magnets contribute to the upward magnetic force but only one magnet contributes to the downward force ensuring the payload does not go flying

7.1 Preliminary Results

The time it took for Payload 4 to block the laser light a fixed distance above was measured for low voltages with two copper tubes on either sides of the payload. These two copper tubes were initially used because the existing prototype had two circular holes cut out on the sides that the tubes could be placed in and easily removed for comparisons between experiments with and without copper.

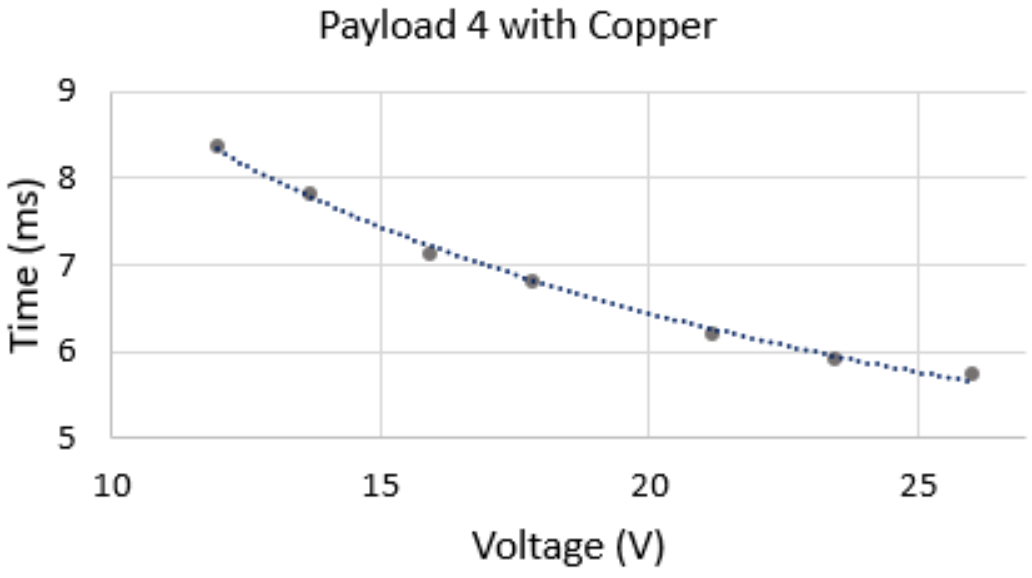

Figure 7.1: Time to travel 6mm (current LIGO operating condition) for Payload 4 at various low voltages applied to coils with exponential fit. Two copper tubes were placed in either sides of the payload.

The exponential fit for this payload with two copper tubes part of the system was:

$$t = 28.744 * v^{-0.499}$$
$$\text{with } R^2 = 0.9955$$

As expected, the dynamics of the system are the same as in the case without copper as the $t \propto v^{-0.5}$ relation can be experimentally verified.

The difference between the time for sustained blocking (time after all oscillations and laser light was continuously blocked in the low voltage setup) in the case without copper and with the two copper tubes was also measured to see whether this eddy current damping had an effect on this system and was an idea worth exploring.

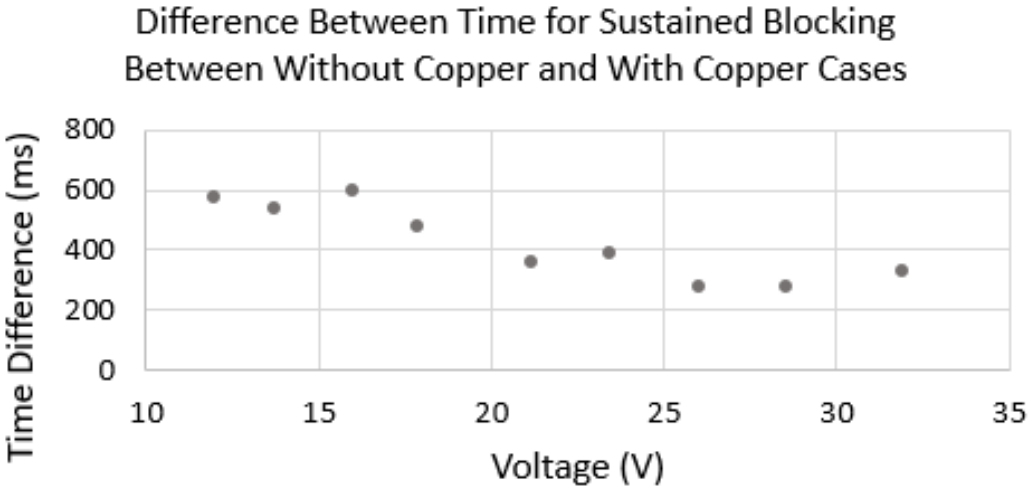

Figure 7.2: Difference between time for sustained blocking of laser light with payload 4 in the case without copper and the case with two copper tubes for low voltage pulses.

While it is difficult to make a confident statement about the trend of the difference in the time for sustained blocking between the case with and without the two copper tubes, it is clear that the copper damping would be a promising way forward since it damps the oscillations of the payloads.

To further pursue this idea and more concretely understand the effect of the copper, Payload 2 was used for the further experiments. Since Payload 2, unlike Payload 4, has no gap between the magnets that laser light can shine through, there are no oscillations resulting in the light unblocked as it shines through the gap.

7.2 Characterizing oscillatory motion

The height of the payload after an initial low voltage pulse was applied was plotted over time along with exponentially decaying sinusoidal fits to understand the oscillatory motion of the payload in a system with and without copper tubes.

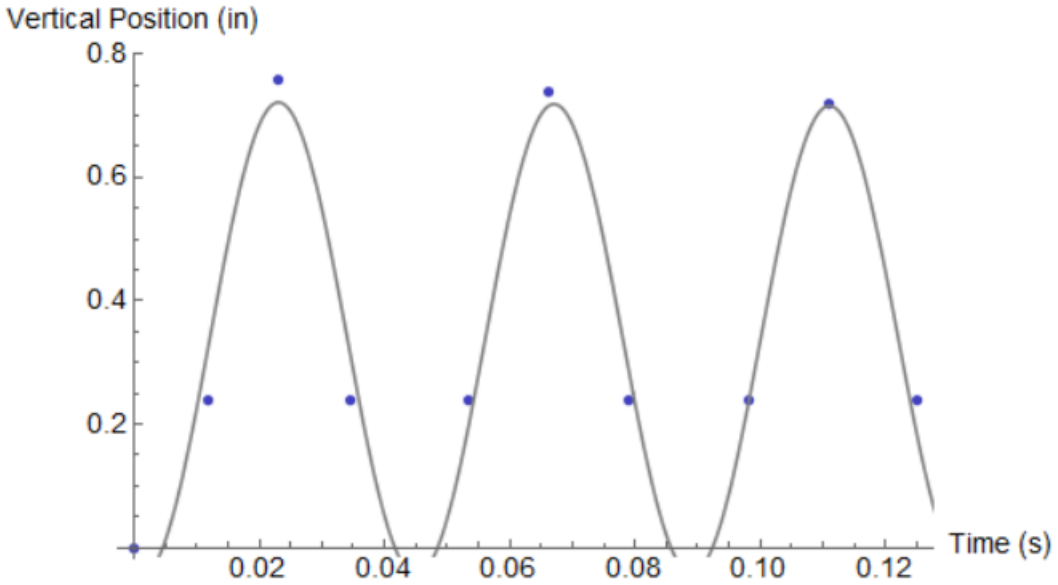

Figure 7.3: Height of the bottom of the payload where 0.0 indicates its starting position versus time. No copper is present in the system.

The fitted exponentially decaying sine wave for this graph was

$$0.385468 * e^{-0.17002*t} * sin(142.844 * t + 4.55731) + 0.338018$$

$$\text{Frequency} = 23Hz$$

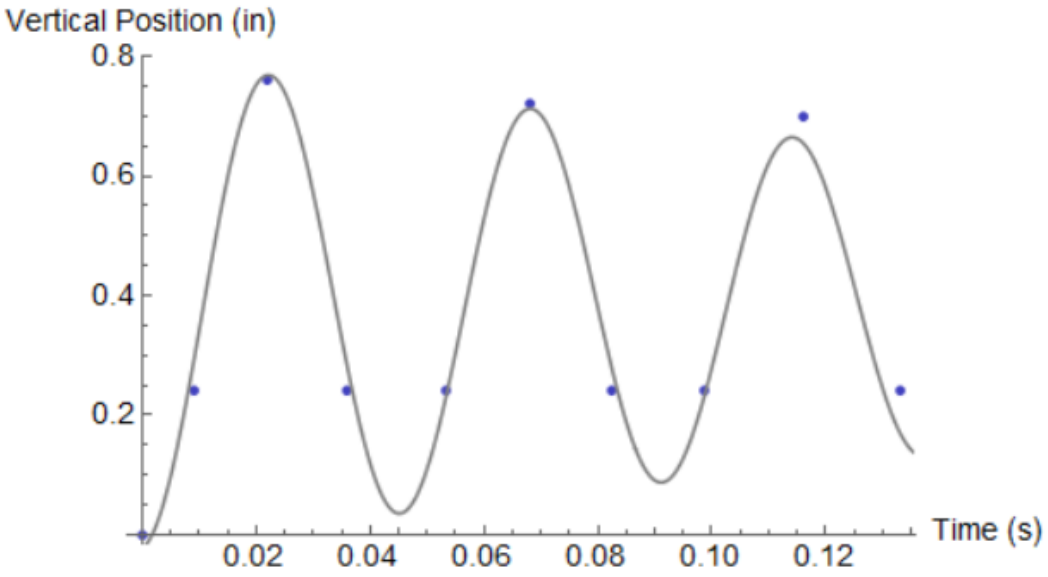

Figure 7.4: Height of the bottom of the payload where 0.0 indicates its starting position versus time. One copper tube is placed in the coil setup on one side of the payload.

The fitted exponentially decaying sine wave for this graph was

$$0.411803 * e^{-3.46399*t} * sin(136.581 * t + 4.80665) + 0.387761$$

Frequency = $22Hz$

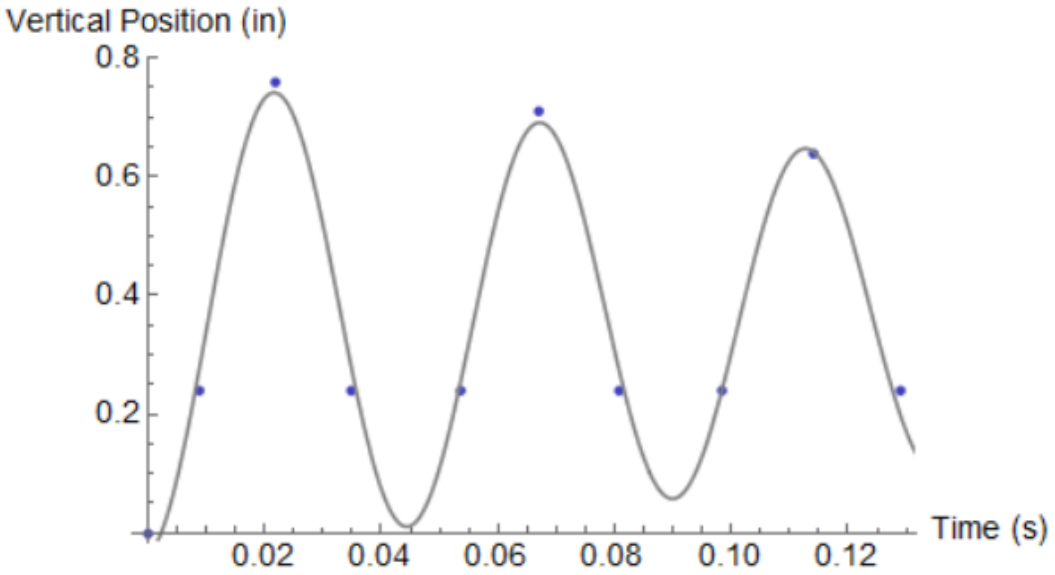

Figure 7.5: Height of the bottom of the payload where 0.0 indicates its starting position versus time. Two copper tubes are placed in the coil setup, one on each side of the payload.

The fitted exponentially decaying sine wave for this graph was

$$0.405653 * e^{-3.14579*t} * sin(137.988 * t + 4.84985) + 0.36294$$
$$\text{Frequency} = 22Hz$$

The frequency of the oscillation in all three cases is essentially the same, as expected. The exponential damping factor is about 18 times larger in the cases with at least one copper tube than in the case with no copper at all, showing that the eddy current damping does significantly slow down the payload as it does not travel as far up or down compared to the case without copper.

It is difficult to distinguish between the case with just one copper tube and the case with two. These results were relatively easy to obtain with the existing setup, but the copper area is quite small compared to the width of the magnet, so it is possible that more magnet overlap with copper would provide more noticeable effects that cannot be discerned in this situation with limited copper.

7.3 Instantaneous Velocity

The main goal of the copper experiments was to understand whether copper damping would be sufficient to make up for the fact that the payload is accelerated upwards

with the magnetic force on two magnets but is not brought back down into the hole between the two coils because there is a magnetic force downward on only the bottom magnet. More specifically, it was important to understand how the amount of copper overlap with the magnets scaled with the damping effect.

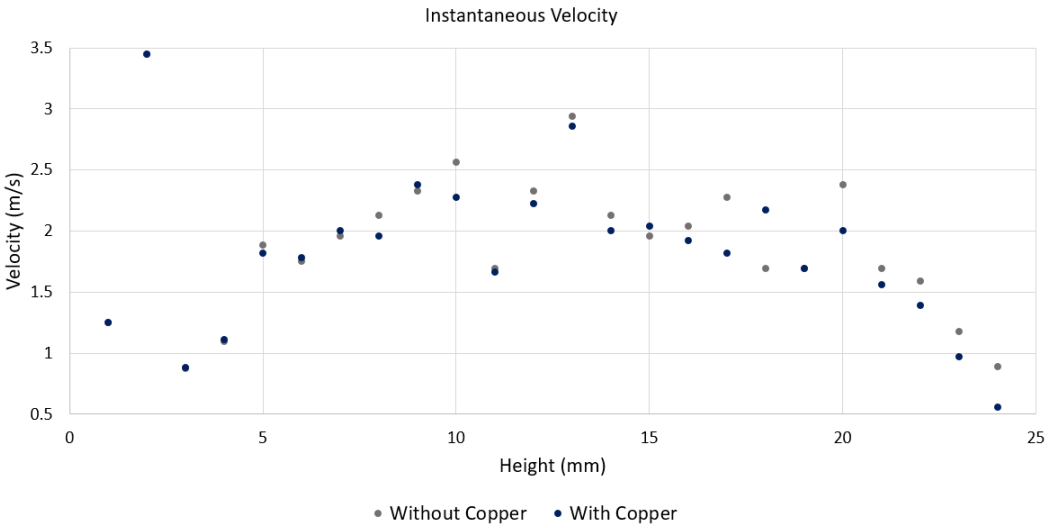

Figure 7.6: Instantaneous velocity of Payload 4 over the entire vertical distance it travels after a low voltage pulse ($30V$) is applied, both without copper and with the two copper tubes on either side of the payload. Data obtained with Lauren Lo Coco.

There are a few outliers in the data, particularly at $2mm$, $11mm$, $13mm$, and $20mm$, likely due to slight measurement errors exacerbated by this plot displaying instantaneous velocity across very short distances. For general conclusions, these data points were eliminated from calculations.

At a high level, the velocity is clearly increasing from $3mm$ to $6mm$, when the top magnet and the bottom magnet are directly overlapping with the top and bottom parts of the coils, respectively. This region corresponds to the initial acceleration that propels the payload upwards. This observation is also consistent with a graph of the average velocity of Payload 4 indicating that the payload is accelerating throughout the entire $6mm$ travel.

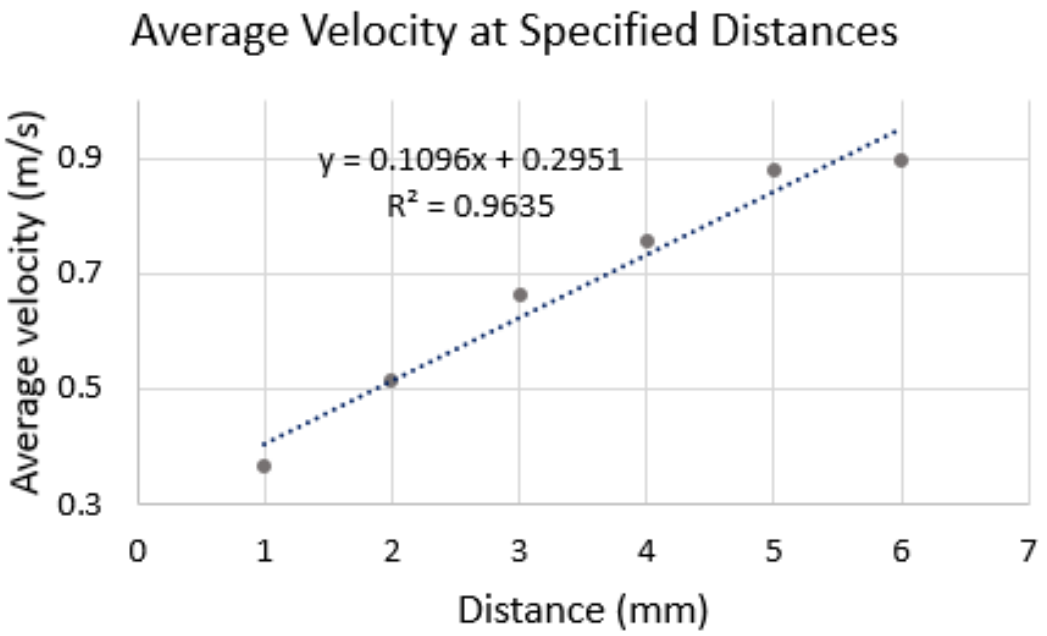

Figure 7.7: Average velocity of Payload 4 for 1*mm* to 6*mm* of travel.

On the instantaneous velocity plot, the bottom magnet begins to directly overlap with the copper tubes at around 13*mm* and leaves the direct overlap region at 18*mm*, which corresponds to a decrease in velocity as can be seen on the graph. From 20*mm* to 25*mm*, the bottom magnet enters and leaves the region of direct overlap with the top coil, so the velocity decreases again as well. Looking at the slope of the velocity decrease in the two cases, the decrease due to the magnetic field of the coil is approximately more than 3.5 times more pronounced than that due to the copper damping, indicating this amount of copper damping with the two copper tubes will not be sufficient to bring the payload back down when higher voltages are applied.

7.4 Future Work

With the current experimental setup and existing PEEK housing for the coils, it is difficult to immediately test other forms of copper damping. However, with a 3D-printed model (currently being designed), more flexibility can be added in the next step to test the effect of wider and taller pieces of copper on the sides of the payload. Currently, the copper tubes are around $\frac{1}{3}$ of the width of the magnets, so increasing the width of the copper would induce more eddy current damping with more direct overlap between the bottom magnet and copper. Since there is no horizontal motion of the payload, there is no reason to make the copper pieces wider than the width of the magnet. Taller copper pieces would again increase the

time of direct overlap between the magnet and the copper, although it is critical to ensure that this interaction region does not begin before the payload has gone up $6mm$, or else the initial acceleration to meet the time specification for blocking will be unintentionally damped.

Chapter 8

CONCLUSION

8.1 Proposed Payload

Payload 4 was ultimately determined to be the optimal payload for the next generation fast shutter system. Important features of this payload include the use of two B842-N52 magnets and a light "flag" mirror. The magnets should be spaced $0.5in$ apart for optimal performance and the starting position of the payloads within the coil should be with the bottom magnet and bottom coil aligned. Furthermore, the mirror should be directly affixed to the top magnet.

8.2 Future Work

Coil Inductance Effects

The inductance of both the coils in parallel is $2.4mH$. Using the model for a series LR circuit with the inductance L and resistance R of the coil (resulting in time constant $\tau = L/R$), the current I through the coils over time t can be modeled as $I = 1 - e^{-Rt/L}$. This relation gives that:

Time (ms)	Percent of Final Current Value
0.25	73
0.5	93
0.75	98
1	99
1.5	99.96
1.9	99.99

Table 8.1: Percent of final current value reached over time, modeling the coils connected in parallel as a series LR circuit for significant times.

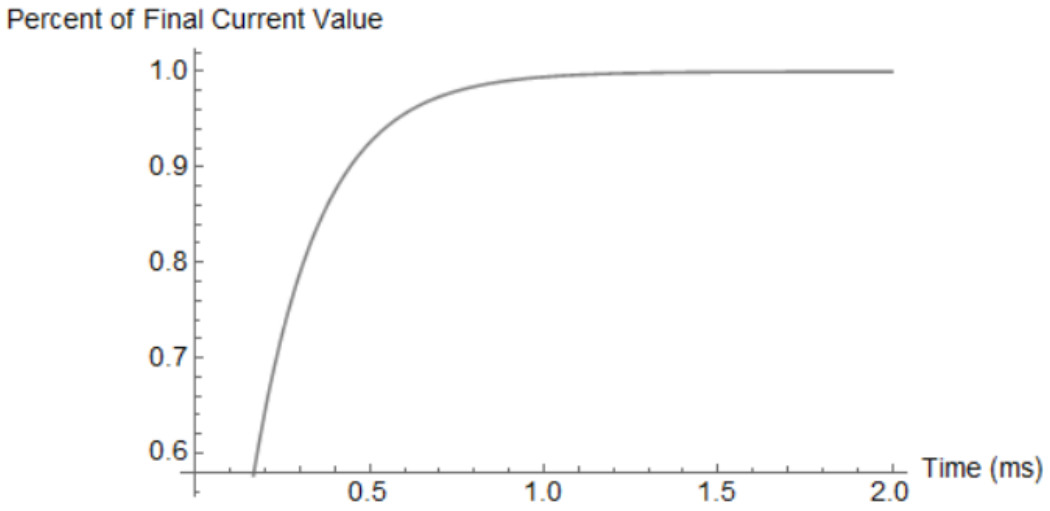

Figure 8.1: Graph of percent of final current value reached over time, modeling the coils connected in parallel as a series LR circuit.

Since the performance goal for this system was to travel $6mm$ in $1ms$, the inductance of the coil does have an impact on the calculations as the current goes from $0A$ to 99% of its final value in that time duration. Furthermore, the rise time of the current when $240V$ is applied (ensuring $6mm$ travel in $1.9ms$ as in current operation) was found to be $1ms$, while lowering the inductance of the coil in circuit simulation reduces the rise time. While this effect can be roughly adjusted for by ensuring the average current is the value desired by increasing the initial voltage applied to the system, the effect of the coil inductance can be properly characterized in future work.

Vacuum Testing

The fast shutter will ultimately perform in vacuum at the LIGO observatories, so it is critical to translate these experiments in air to a vacuum setup and verify their operations before installing. It is particularly important to ensure that damping caused by air is accounted for in our current results.

Real Mirror

Currently, these experiments have been conducted with a light "flag" intended to serve as a model for a light thin mirror. The flag has additionally been affixed to the top of the upper magnet for these experiments, but the final design proposal has the magnet directly affixed on the upper magnet. The design of such a mirror along with associated costs will need to be investigated to understand how thin the mirror

can be and obtain a realistic number of its weight. It will also be important to ensure that the slight asymmetry of having a mirror on one side of the top magnet does not cause any issues.

Other Variables

While the performance of Payload 4 is on par with current LIGO operating conditions, increasing the number of turns of the coil and experimenting with the coil geometry could be variables that are adjusted to travel 6*mm* even faster or with less voltage applied to the coils. At this current point, it is likely not necessary to adjust these variables other than aiming to minimize the distance between the magnets and coil for stronger interaction.

Copper Damping

As explained in the eddy current damping with copper chapter, a new 3D-prototype is being built so that the effect of copper damping can be further understood. Payload 4 is the best payload experimented with in terms of achieving the performance goals, so finalizing the copper damping so that the payload comes back down is critical for usage in LIGO laboratories.

Once the damping mechanism is verified and finalized, a new test prototype can be built to test with high voltages and in vacuum, before hopefully being installed at the observatories to replace the first generation fast shutter system!

Use of a Wider Magnet

During high voltage experiments, the payload does not come back into the guiding channel without any additional damping since the initial acceleration is due to the upward force on two magnets while a downward force acts on only one magnet to bring the payload back down.

To combat this issue without copper or magnetic damping, just one magnet could be used at the bottom of the payload, similar to Payload 3. This payload was initially dismissed compared to Payload 4 because the initial force on two magnets part of Payload 4 resulted in a faster block time than with just one magnet part of Payload 3. However, if the magnet was twice as wide (as was the guiding channel so the payload would fit), the initial net direct overlap between magnets and coils resulting in an upward force would be the same between Payload 4 and this payload with one wider magnet. A possible such magnet that could be used is the BX042-N52 magnet with dimensions 1in x $\frac{1}{4}$in x $\frac{1}{8}$in, magnetization direction thru thickness, and weight

3.84g, the same weight as the B882G-N52 magnet used as part of Payload 1.

Furthermore, the problem of bringing the payload back down would also not be an issue. In the one magnet scenario, the force on one magnet brings the payload up and the force on that same magnet when it reaches the top coil brings the payload down. This behavior has been verified with high voltage pulses and the payload does not going flying.

To further characterize this payload and verify it meets the design specifications, a 3D model of an encasing to wrap the coil around and fit the payload is currently being built.

BIBLIOGRAPHY

Abbott, Richard and Peter Fritschel (2015). *Ultra-fast Mechanical Shutter*. US Patent 0331232.

Fritschel, Peter and Richard Abbott (2014). “Ultra-fast Optical Shutter Design”.

Sanchez, Eduardo (2016). “Fast Shutter, Coil Former Assembly”.